03

Analysis of Wave Focusing by Axisymmetric Magneto-Dielectric Maxwell and Mikaelian Lenses Using a Modified Hybrid Projection Method

© M.M. Kushneryov[1,2], E.I. Semernya[3], S.P. Skobelev[1,2,¶]

[1] Moscow Institute of Physics and Technology (National Research University), Dolgoprudny, Moscow Region, Russia
[2] PAO „Radiofizika “, Moscow, Russia
[3] Moscow Aviation Institute National Research University, Moscow, Russia

¶ e-mail: s.p.skobelev@mail.ru

Received May 03 August 2024
Revised December 23, 2024
Accepted December 28, 2024

A problem of electromagnetic wave scattering on axisymmetric inhomogeneous magneto-dielectric objects is considered. A modified algorithm based on the hybrid projection method is developed for providing an option of taking into account not only variable profile of dielectric permittivity of the object as it took place in the previous publications, but also variable profile of magnetic permeability. The new modification is applied for comparative analysis of plane wave focusing by a hemispherical Maxwell lens and a cylindrical Mikaelian lens with axial symmetry. The results obtained with use of the hybrid projection method are compared to the results obtained by the method of surface integral equations applied to layered models of the lenses. Some results demonstrating the influence of matching the lens surfaces to free space by means of using identical profiles of permittivity and permeability on the quality of focusing are presented and discussed.

Keywords: inhomogeneous media, wave scattering, Maxwell lens, Mikaelian lens, numerical methods.

DOI: 10.61011/EOS.2025.01.60563.6960-24

Introduction

The well-known „fisheye“ Maxwell lens [1,2] and Mikaelyan lens [3,4] continue to be of interest to the researchers and development engineers in optics and antenna technology up to the present day. Expression of the interest takes place both in development of new technologies for manufacture of these lenses on the basis of artificial dielectric [5–7] with use of three-dimensional printing of the dielectric elements [8], and in development of new numerical methods the effective design of the Maxwell and Mikaelian lenses and for analysis of their characteristics [9,10].

The analysis of the focusing properties of Maxwell and Mikaelian lenses in the frame of approximations of geometric optics is described in a few books, e.g. in [11–13], and in a number of other publications. Analysis of the dielectric lenses under consideration in a rigorous statemen of the problem was carried out by various numerical methods, including methods implemented in the well-known CST Microwave Studio Suite package, such as in jcite7, the finite element method jcite14 and the hybrid projection method (HPM) in [9,10], where positive features of the latter in comparison with other methods are described.

The results obtained in [9,10] in the process of numerical analysis of axisymmetric purely dielectric Maxwell and Mikaelian lenses demonstrate that focusing of an incident plane wave is accompanied with partial reflection from flat the surfaces in both lenses and significant field oscillations inside the Mikaelian lens. The indicated effects are caused by the mismatch of the lens surfaces with free space, leading to reduction in quality of focusing. One of the possible ways to reduce reflections from the lens surface is to use magneto-dielectric materials with a wave resistance equal to the wave resistance of free space.

The purpose of the present study includes development of a new HPM modification, which allows taking into account not only the variable profile of dielectric permittivity in an axisymmetric body in general case, but also the variable profile of magnetic permeability, as well as application of the indicated modification for a comparative analysis of the focusing properties of a hemispherical Maxwell lens and a cylindrical Mikaelian lens made of a magneto-dielectric material.

HPM modification

Let's consider an inhomogeneous magneto-dielectric body of revolution located in free space in Cartesian coordinates x, y, z and spherical coordinates r, θ, φ, as shown in Fig. 1. The indicated body is characterized by relative permittivity $\varepsilon(r, \theta)$ and relative permeability $\mu(r, \theta)$, depending on the radial coordinate r and the angular coordinate θ. The body of revolution under consideration is assumed to be excited by a harmonic homogeneous plane electromagnetic wave of specified amplitude and

polarization, and the aim of the problem consists in determining both the electromagnetic field passed inside the body and the field scattered into free space.

According to the approach described in jcite9, when solving the problem of exciting a purely dielectric body of revolution, the body in question is surrounded by a virtual sphere of radius a with the center located at the origin, as shown in Fig. 1. The transverse components of the electric and magnetic field strength vectors outside the sphere in $r \geq a$ region are further represented as expansions in terms of spherical wave functions:

$$\mathbf{E}_\tau(r,\theta,\varphi) = \frac{1}{kr}\sum_{q=0}^{\infty}\sum_{m=-q}^{q}\left\{\left[A_{1q}^m\psi_q(kr) + R_{1q}^m\xi_q(kr)\right]\mathbf{Y}_{1q}^m + \left[A_{2q}^m\psi_q'(kr) + R_{2q}^m\xi_q'(kr)\right]\mathbf{Y}_{2q}^m\right\}, \tag{1}$$

$$\mathbf{H}_\tau(r,\theta,\varphi) = -\frac{i}{\eta_0 kr}\sum_{q=0}^{\infty}\sum_{m=-q}^{q}\left\{\left[A_{1q}^m\psi_q'(kr) + R_{1q}^m\xi_q'(kr)\right]\mathbf{Y}_{2q}^m + \left[A_{2q}^m\psi_q(kr) + R_{2q}^m\xi_q(kr)\right]\mathbf{Y}_{1q}^m\right\}, \tag{2}$$

where A_{1q}^m and A_{2q}^m — known amplitudes of the incident transverse-electric (TE) and transverse-magnetic (TM) waves, respectively; R_{1q}^m and R_{2q}^m — unknown amplitudes of TE- and TM-waves of scattered field; $\psi_q(\ldots)$ — Riccati-Bessel functions of q-th order, $\xi_q(\ldots)$ — Riccati-Hankel functions of the first kind of q-th order corresponding to the dependence on time $e^{-i\omega t}$; the primes on these functions denote the derivatives with respect to the entire argument; $k = 2\pi/\lambda$ — wave number; λ — wavelength in free space; η_0 — wave resistance of free space; $\mathbf{Y}_{jq}^m(\theta,\varphi)$ — ortho-normalized transverse vector spherical functions corresponding to TE ($j = 1$)- and TM ($j = 2$)-waves defined in [9].

The transverse components of the electric and magnetic field strength vectors inside the sphere at $0 \leq r \leq a$ are also represented as expansions in terms of transverse wave functions:

$$\mathbf{E}_\tau(r,\theta,\varphi) = \sum_{q=0}^{\infty}\sum_{m=-q}^{q}\left[E_{1q}^m(r)\mathbf{Y}_{1q}^m + E_{2q}^m(r)\mathbf{Y}_{2q}^m\right], \tag{3}$$

$$\mathbf{H}_\tau(r,\theta,\varphi) = \frac{1}{\eta_0}\sum_{q=0}^{\infty}\sum_{m=-q}^{q}\left[H_{1q}^m(r)\mathbf{Y}_{2q}^m + H_{2q}^m(r)\mathbf{Y}_{1q}^m\right] \tag{4}$$

with variable coefficients $E_{jq}^m(r)$ and $H_{jq}^m(r)$, depending on the radial coordinate r.

Substitution of the transverse components (3) and (4) into Maxwell equations

$$\nabla\times\mathbf{H} + \frac{ik\hat{\varepsilon}}{\eta_0}\mathbf{E} = 0, \tag{5}$$

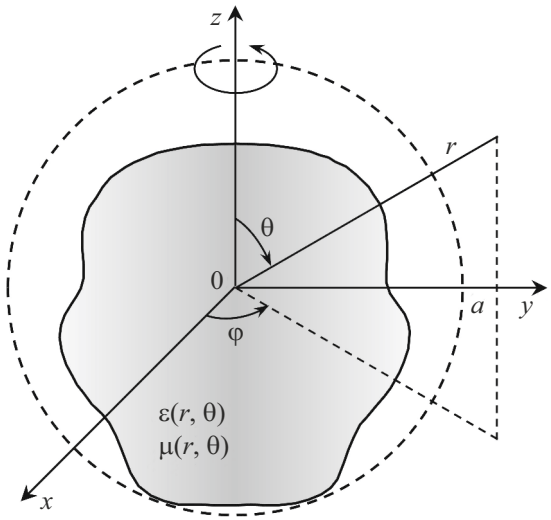

Figure 1. Geometry of the problem in general case of magneto-dielectric body of revolution.

$$\nabla\times\mathbf{E} - ik\eta_0\hat{\mu}\mathbf{H} = 0, \tag{6}$$

written for the fields inside the sphere, where $\hat{\varepsilon} = \varepsilon(r,\theta)$, $\hat{\mu} = \mu(r,\theta)$ inside the body and $\hat{\varepsilon} = 1$, $\hat{\mu} = 1$ outside the body of revolution allows getting the representations for longitudinal (radial) components of the electrical and magnetic fields as

$$E_r(r,\theta,\varphi) = \frac{1}{kr\hat{\varepsilon}}\sum_{q=0}^{\infty}\sum_{m=-q}^{q}\alpha_q H_{1q}^m(r)Y_{3q}^m, \tag{7}$$

$$H_r(r,\theta,\varphi) = -\frac{1}{\eta_0 kr\hat{\mu}}\sum_{q=0}^{\infty}\sum_{m=-q}^{q}\alpha_q E_{1q}^m(r)Y_{3q}^m, \tag{8}$$

where $\alpha_q = \sqrt{q(q+1)}$ and $Y_{3q}^m(\theta,\varphi)$ — ortho-normalized transverse scalar spherical functions defined in [9].

Electric fields (1) and (3), as well as magnetic fields (2) and (4) must be continuous on the sphere surface. The indicated conditions give the following relations between the expansion coefficients:

$$A_{1p}^m\psi_p(ka) + R_{1p}^m\xi_p(ka) = kaE_{1p}^m(a), \tag{9}$$

$$A_{2p}^m\psi_p'(ka) + R_{2p}^m\xi_p'(ka) = kaE_{2p}^m(a), \tag{10}$$

$$iA_{1p}^m\psi_p'(ka) + iR_{1p}^m\xi_p'(ka) = -kaH_{1p}^m(a), \tag{11}$$

$$iA_{2p}^m\psi_p(ka) + iR_{2p}^m\xi_p(ka) = -kaH_{2p}^m(a). \tag{12}$$

Projection of Maxwell's equations (5) and (6) onto conjugate transverse vector functions $Y_{jp}^{m*}(\theta,\varphi)$ with taking into account the longitudinal components (7) and (8), as described in jcite9, leads to a system of ordinary differential equations

$$k\sum_{q=|m|}^{\infty}\left[\left(W_{\varepsilon pq} - \frac{\alpha_p\alpha_q}{kr^2}Z_{\mu pq}\right)U_{1q} - X_{\varepsilon pq}U_{2q}\right] + i\frac{dV_{1p}}{dr} = 0, \tag{13}$$

$$k\sum_{q=|m|}^{\infty}\left(X_{\varepsilon pq}U_{1q}+W_{\varepsilon pq}U_{2q}\right)-i\,\frac{dV_{2p}}{dr}=0, \tag{14}$$

$$i\,\frac{dU_{1p}}{dr}+k\sum_{q=|m|}^{\infty}\left(W_{\mu pq}V_{1p}+X_{\mu pq}V_{2q}\right)=0, \tag{15}$$

$$-i\,\frac{dU_{2p}}{dr}+k\sum_{q=|m|}^{\infty}\left[-X_{\mu pq}V_{1q}+\left(W_{\mu pq}-\frac{\alpha_p\alpha_q}{kr^2}\,Z_{\varepsilon pq}\right)V_{2q}\right]=0 \tag{16}$$

for functions $U_{jq}(r)=krE^m_{jq}(r)$ and $V_{jq}(r)=krH^m_{jq}(r)$ ($j=1,2$, m — integer number), where

$$W_{\xi pq}(r)=\int_0^{\pi}\xi\mathbf{T}^{m*}_{1p}\cdot\mathbf{T}^{m}_{1q}\sin\theta d\theta=\int_0^{\pi}\xi\mathbf{T}^{m*}_{2p}\cdot\mathbf{T}^{m}_{2q}\sin\theta d\theta, \tag{17}$$

$$X_{\xi pq}(r)=-\int_0^{\pi}\xi\mathbf{T}^{m*}_{1p}\cdot\mathbf{T}^{m}_{2q}\sin\theta d\theta=\int_0^{\pi}\xi\mathbf{T}^{m*}_{2p}\cdot\mathbf{T}^{m}_{1q}\sin\theta d\theta, \tag{18}$$

$$Z_{\xi pq}(r)=\int_0^{\pi}\frac{1}{\xi}\,T^{m*}_{3p}T^{m}_{3q}\sin\theta d\theta, \tag{19}$$

$\xi=\hat{\varepsilon}$, $\hat{\mu}$, and functions $\mathbf{T}^m_{jq}(\theta)$ and $T^m_{3q}(\theta)$, orthonormalized in $0\le\theta\le\pi$ region, are multipliers in functions $\mathbf{Y}^m_{jq}(\theta,\varphi)$ and $Y^m_{3q}(\theta,\varphi)$, respectively [9]. It can be noted that the system of equations (9)–(12) for four sets of unknown coefficients differs from the similar system obtained in [9] for three sets of unknown coefficients in case of a purely dielectric bodies of revolution.

The differential equations (13)–(16) are solved by a 1D finite element method. The unknown variable coefficients from (13)–(16) are expressed as expansions

$$U_{jq}(r)=\sum_{n=1}^{N}U_{jnq}f_n(r), \tag{20}$$

$$V_{jq}(r)=\sum_{n=1}^{N}V_{jnq}f_n(r), \tag{21}$$

where U_{jnq} and V_{jnq} — unknown constant coefficients, N — number of nodes with coordinates $r_n=n\Delta$, $\Delta=a/N$ and $f_n(r)$ — triangular functions with vertices located in these nodes. Projection of differential equations (13)–(16) on triangular functions $f_{n'}(r)$ results in the following system of linear algebraic equations (SLAE):

$$\sum_{n=1}^{N}\sum_{q=|m|}^{\infty}\left\{\left(\tilde{W}^{pq}_{\varepsilon n'n}-\tilde{Z}^{pq}_{\mu n'n}\right)U_{1nq}-\tilde{X}^{pq}_{\varepsilon n'n}U_{2nq}\right\}$$

$$-i\sum_{n=1}^{\infty}K^{(1)}_{n'n}V_{1np}+R^m_{1q}\xi'_p(ka)\delta_{n'N}=A^m_{1p}\psi'_p(ka)\delta_{n'N}, \tag{22}$$

$$\sum_{n=1}^{N}\sum_{q=|m|}^{\infty}\left(\tilde{X}^{pq}_{\varepsilon n'n}U_{1nq}+\tilde{W}^{pq}_{\varepsilon n'n}U_{2nq}\right)-i\sum_{n=1}^{N}K^{(2)}_{n'n}V_{2np}=0, \tag{23}$$

$$i\sum_{n=1}^{N}K^{(2)}_{n'n}U_{1np}+\sum_{n=1}^{N}\sum_{q=|m|}^{\infty}\left(\tilde{W}^{pq}_{\mu n'n}U_{1nq}+\tilde{X}^{pq}_{\mu n'n}U_{2nq}\right)=0, \tag{24}$$

$$i\sum_{n=1}^{\infty}K^{(1)}_{n'n}U_{2np}+\sum_{n=1}^{N}\sum_{q=|m|}^{\infty}\left\{-\tilde{X}^{pq}_{\varepsilon n'n}V_{1nq}+\left(\tilde{W}^{pq}_{\varepsilon n'n}-\tilde{Z}^{pq}_{\mu n'n}\right)V_{2nq}\right\}-iR^m_{2q}\xi'_p(ka)\delta_{n'N}=iA^m_{2p}\psi'_p(ka)\delta_{n'N}, \tag{25}$$

where $\delta_{n'n}$ — Kronecker symbol,

$$\tilde{W}^{pq}_{\xi n'n}=k\int_0^a f_{n'}f_nW_{\xi pq}dr, \tag{26}$$

$$\tilde{X}^{pq}_{\xi n'n}=k\int_0^a f_{n'}f_nX_{\xi pq}dr, \tag{27}$$

$$\tilde{Z}^{pq}_{\xi n'n}=\frac{\alpha_p\alpha_q}{k}\int_0^a\frac{f_{n'}f_n}{r^2}\,Z_{\xi pq}dr, \tag{28}$$

$$K^{(1)}_{n'n}=\int_0^a\frac{df_{n'}}{dr}\,f_ndr, \tag{29}$$

$$K^{(2)}_{n'n}=\int_0^a f_{n'}\,\frac{df_n}{dr}\,dr. \tag{30}$$

matrix elements and $n'=1,2,\ldots,N$. Integration by parts of the last term in the left part of equation (13) and the first term in the left part of equation (16) was carried out with taking into account the relations (11) and (10), respectively. The relations (9) and (12) give two more algebraic equations

$$U_{1Np}-\xi_p(ka)R^m_{1p}=A^m_{1p}\psi_p(ka), \tag{31}$$

$$V_{2Np}+i\xi_p(ka)R^m_{2p}=-iA^m_{2p}\psi_p(ka), \tag{32}$$

where $U_{1Np}=kaE^m_{1p}(a)$ and $V_{1Np}=kaH^m_{1p}(a)$. Account for L of the first terms by index q in expansions (1)–(4) and two equations (31) and (32) defines the algebraic system order equal $(4N+2)L$, for each azimuthal index m. The matrix of the system has a block tridiagonal structure, an example of which, corresponding to $N=4$, is shown in Fig. 2, where gray squares indicate completely filled blocks; white areas contain only zero elements, and squares with diagonal lines contain non-zero elements only on the main diagonal.

The expansion coefficients obtained after solving the algebraic system are then used to calculate the field at specific points in space both inside and outside the virtual sphere introduced above.

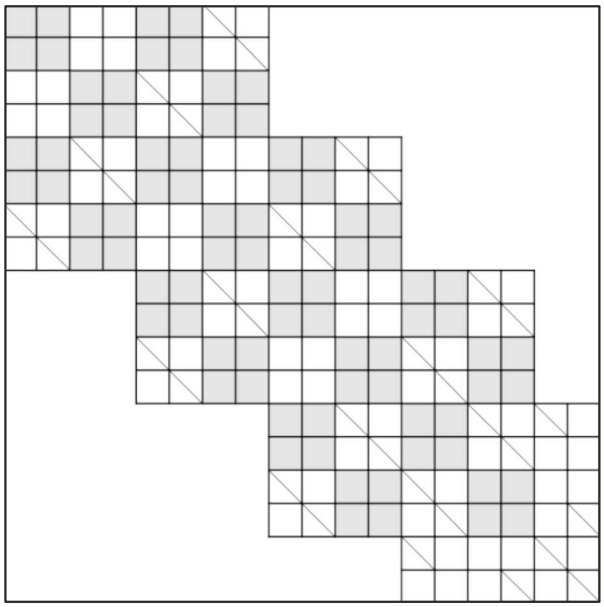

Figure 2. Structure of SLAE matrix at $N = 4$, where each block consists of $L \times L$ elements.

Numerical results

The HPM modification developed above was implemented in two computer programs in MatLab language designed for comparative numerical analysis of the focusing properties of hemispherical Maxwell „fisheye“ lens and cylindrical Mikaelian lens.

Geometry in Maxwell lens problem is illustrated in Fig. 3. The lens radius in this case coincides with the radius a of the virtual sphere. The radial profile of the refractive index of the lens is determined by well-known formula $n(r) = 2/[1 + (r/a)^2]$ [11–13]. The profile of dielectric permittivity in a purely dielectric lens, where the relative magnetic permeability is equal to unity, i.e. $\mu(r) = 1$, is expressed as $\varepsilon(r) = n^2(r)$ [9,14]. The case of a magneto-dielectric lens with $\varepsilon(r) = \mu(r) = n(r)$, considered below, is of interest from the viewpoint of the lens matching with free space.

The lens is supposed to be irradiated by a circularly polarized planar wave propagating in the negative direction of the $z$axis. The electric field of the incident wave can be represented as

$$\mathbf{E}^i(\mathbf{r}) = (\mathbf{e}_x + i\mathbf{e}_y)e^{-ikz}, \qquad (33)$$

where $\mathbf{e}_x$ and $\mathbf{e}_y$ — unit vectors corresponding to Cartesian coordinates. Such an excitation corresponds to only one azimuthal harmonic with index $m = 1$ in the representation of fields (1)−(4), (7) and (8). The expansion coefficients corresponding to the incident wave in (1) and (2) are determined by the formulae

$$A^1_{1q} = 2(-i)^{q+1}\sqrt{(2q+1)\pi}, \quad A^1_{2p} = -A^1_{1q}.$$

The basic details of computations of matrix elements (26)−(30) are discussed in jcite9, where formulae are also provided to calculate the field distribution along the lens axis, which is of primary interest here for analysis of focusing.

The program verification, as in [9], was carried out in several ways, including checking of convergence of the results with increase of N and L, using the optical theorem [15] and comparing the results of the new programs with the results obtained by other methods. Since the new program makes it possible to calculate purely dielectric lenses by specifying $\mu(r) = 1$ in the input data list, it was possible to observe coincidence of the results of operation with the appropriate results of the previous version of the program, developed according to the algorithm described in [9].

The results of computation obtained with the use of the new program to determine the field on the axis of a dielectric and magneto-dielectric Maxwell lens of radius $a = 2.5\lambda$, obtained at $N = 125$ and $L = 41$, are shown in Fig. 4 by a solid line. The presented results are compared here with the results obtained by the method of surface integral equations (IE), implemented in the CST Microwave Studio Suite using a layered lens model. The latter was formed by five hemispherical layers, i.e. the continuous refractive index profile $n(r)$, indicated above, was replaced by a stepped profile. The refraction index of each layer was found from the formula $n_i = n(r_i)$, where $r_i = (l - 1/2)a/5$ and $l = 1, 2, \ldots, 5$. The results shown by the dashed line were obtained using more than 35,000 triangular cells in a grid generated on the outer surface of the and on the inner boundaries of the layers. The calculation time turned out to be almost 6 times longer than the computation time with the new program. The comparisons show that the results obtained by these two methods match well in the focus area and outside the lens,

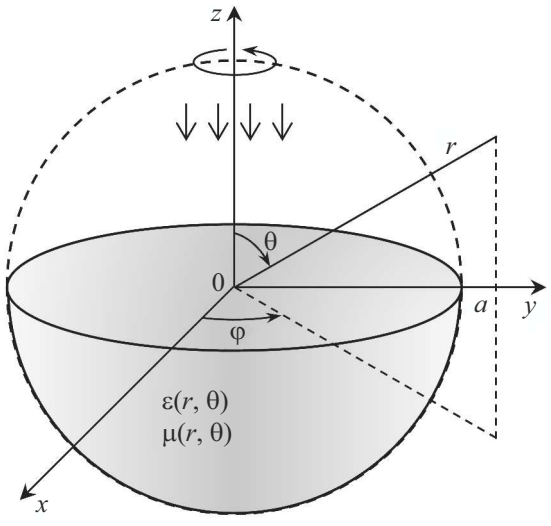

Figure 3. Geometry of the problem for hemispherical Maxwell lens.

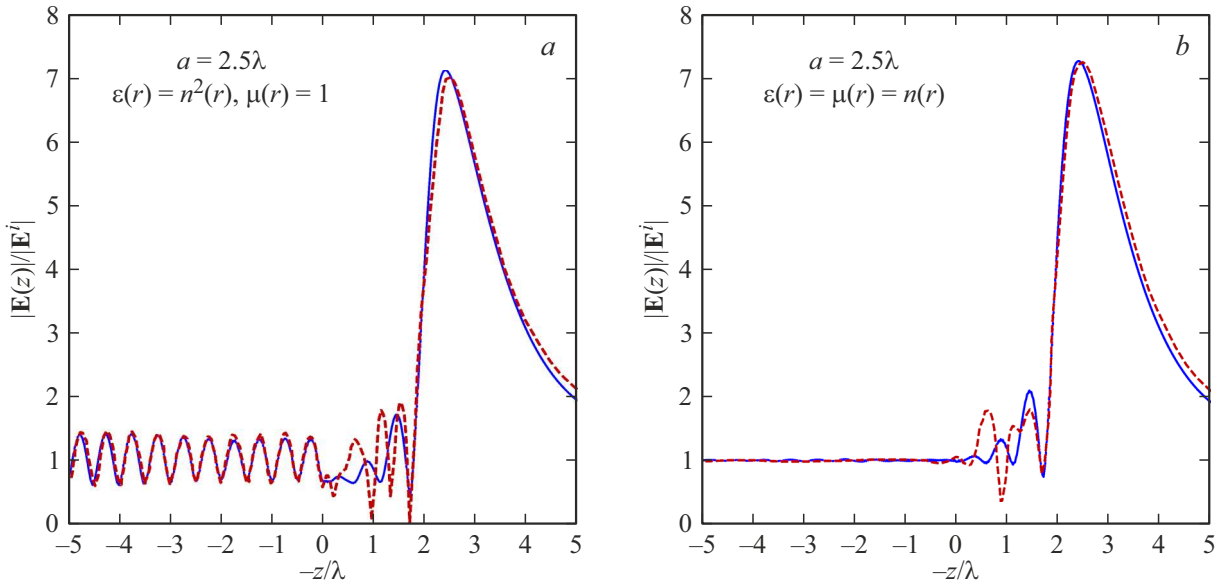

Figure 4. Comparison of the results obtained by the HPM and the method of surface integral equations for dielectric (a) and magneto-dielectric (b) Maxwell lenses with radius $a = 2.5\lambda$.

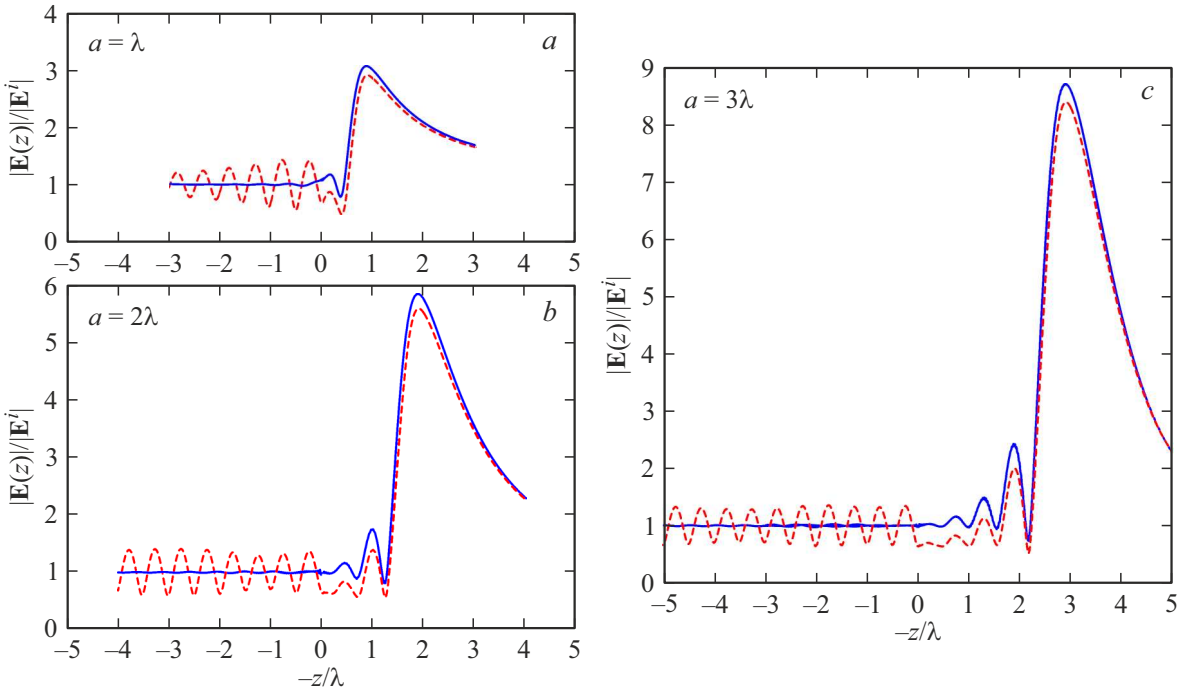

Figure 5. Field distribution along the axis of a hemispherical Maxwell lens of various radii: solid lines — magneto-dielectric lens, dashed lines — dielectric lens.

but have more noticeable differences at a relatively low level inside the lens. These discrepancies can be explained by the differences in the continuous and stepwise refractive index profiles of the lens.

The field distributions for a Maxwell lens with radius $a = \lambda$, 2λ and 3λ are shown in Fig. 5. The results were obtained at $N = 50$, $L = 25$ in the first case, $N = 100$, $L = 35$ in the second case and $N = 150$, $L = 45$ in the third case. We see that the use of a magneto-dielectric material makes it possible to almost completely eliminate the wave reflection from the flat part of the lens surface, which leads to increased field level in the focusing area compared to the case of a purely dielectric lens. It can also be seen that this increase rises with growing of the lens radius.

Geometry of the problem for a cylindrical Mikaelian lens with radius r_c and half height h is provided in

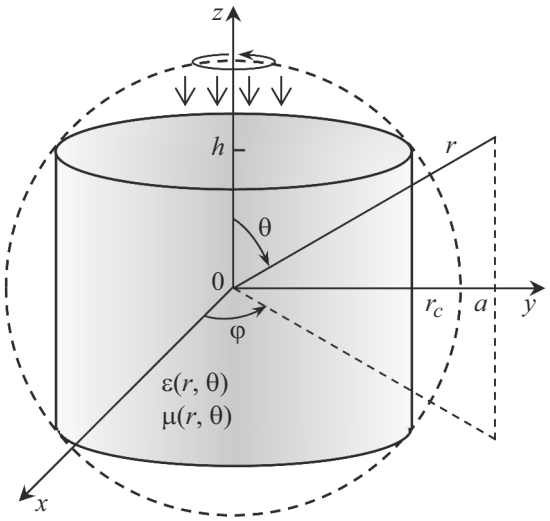

Figure 6. Geometry of the problem for a cylindrical Mikaelian lens

Fig. 6. As it is a well-known (see for example, [3,11,13]), the lens refractive index profile is determined by formula $n(p) = n_0/\cos h(\pi\rho/2h_c)$, where $\rho = r\sin\theta$ — distance from the axis to the observation point, $n_0 = n(0)$ — refractive index on the axis and $h_c = 2h$ — full height of the lens. Further, it is supposed that $n(r_c) = 1$ and respectively $n_0 = \cos h(\pi r_c/2h_c)$. As in the previous case, the lens is irradiated by a circularly polarized plane wave with field (33).

The operation of the Matlab program, designed for analysis of the lens in question, was checked in the same way as in the case of the Maxwell lens. In particular, the results obtained with use of the new program for $\mu(r) = 1$ coincided with the results obtained with use of the previous version for the case of a purely dielectric lens [10].

The field distributions along the axis of the dielectric and magneto-dielectric Mikaelian lenses with parameters $r_c = h = 2.5\lambda$ and $n_0 = 1.3246$ are represented in Fig. 7 by solid lines. The results were obtained at $N = 175$ and $L = 45$. The dashed lines, also shown in Fig. 7, correspond to a layered model of the Mikaelian lens of the same dimension, formed by five layers. Refraction index of l-th layer was determined as $n_l = n(p_l)$, where $\rho_l = (l - 1/2)r_c/5$ and $l = 1, 2, \ldots, 5$. The results were obtained by the method of surface IE with use of 45 000 triangular cells in a grid generated on the outer surface of the lens and on the inner cylindrical boundaries of the layers. The computation took more than 7 times longer than the time taken with use of the new HPM-based program. The results show that both the original and layered lenses are focusing, but the maximum field level in the focus area in the case of the layered lens is lower than in the case of the original lens. It can be expected that increase in the number of layers, corresponding to a more accurate stepwise approximation of the refractive index profile, will lead to enhancement of the field level in the focus. However, this would require higher volume of the PC memory and longer computation time.

The results of computation with use of the new program for the Mikaelian lens with different values of the lens parameters $r_c = h$ are shown in Fig. 8. The computations were performed at $N = 70$, $L = 29$ in case $r_c = h = \lambda$, $N = 140$, $L = 39$ in case $r_c = h = 2\lambda$ and $N = 190$, $L = 49$ in case $r_c = h = 3\lambda$. The results show that, as in case of the Maxwell lens, the use of a magneto-dielectric material in the Mikaelian lens makes it possible to completely eliminate reflections from the input plane (on which the wave falls) and interference of the waves along the axis inside the lens. However, the increase in the maximum field level in the focus area due to the indicated improvement in matching with free space is not so noticeable here as it takes place in the case of the Maxwell lens. This is explained by the fact that locally plane waves corresponding to geometric-optical beams coming into focus of the Maxwell lens do not have any reflections in any direction of arrival due to unit value of the refractive index on the spherical part of the surface. The Mikaelian lens is ideally matched only for the axial direction, and the beams coming into focus at a nonzero angle to the axis will experience reflections, albeit with a lower amplitude than for a purely dielectric lens. By comparing the focusing properties of the Maxwell lens (Figs. 4 and 5) and Mikaelian lens (Figs. 7 and 8) of the same transverse dimensions we also see that the second lens provides a higher field level in the focus area than the first one. Another difference is that the maximum field level of the Mikaelian lens is slightly shifted from the geometric-optical focus outward, while that of the Maxwell lens is shifted — inward, similar to that of the Luneburg lens [16].

Conclusion

Thus, the present paper is devoted to solving the problem of scattering of electromagnetic waves on axisymmetric inhomogeneous magneto-dielectric objects. The problem was solved using the HPM modified for the purpose of accounting for not only the variable profile of dielectric permittivity of the object, as it was in the case of the previous studies, but also the variable profile of the magnetic permeability.

The new modification developed for a general case of excitation of an object with generatrix of an arbitrary shape was implemented in two Matlab programs used for comparative analysis of focusing of a circularly polarized plane wave by a hemispherical Maxwell lens and by a cylindrical Mikaelian lens with axial symmetry during wave propagation in the axial direction. The effectiveness of the method and operation of the corresponding programs were tested in several ways described earlier in [9,10], including a comparison of the results of his work with the results obtained by the method of surface integral equations applied to multilayer models of the Maxwell and Mikaelian lenses.

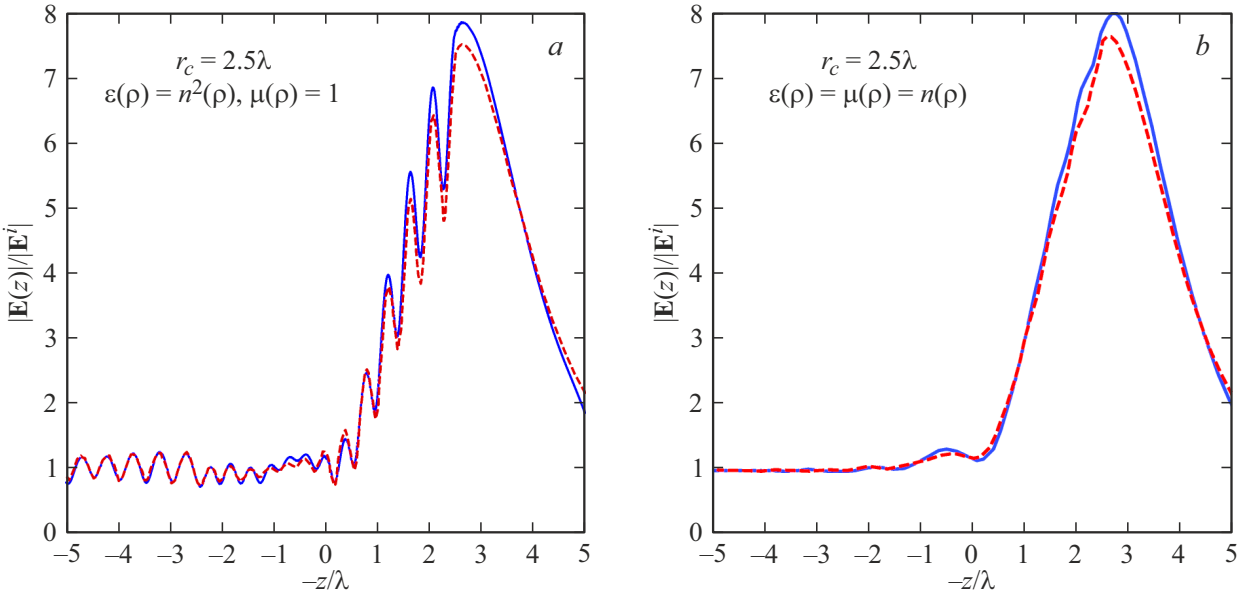

Figure 7. Comparison of the results obtained by the HPM and by the surface integral equation method for dielectric (a) and magneto-dielectric (b) Mikaelian lenses with radius $r_c = h = 2.5\lambda$.

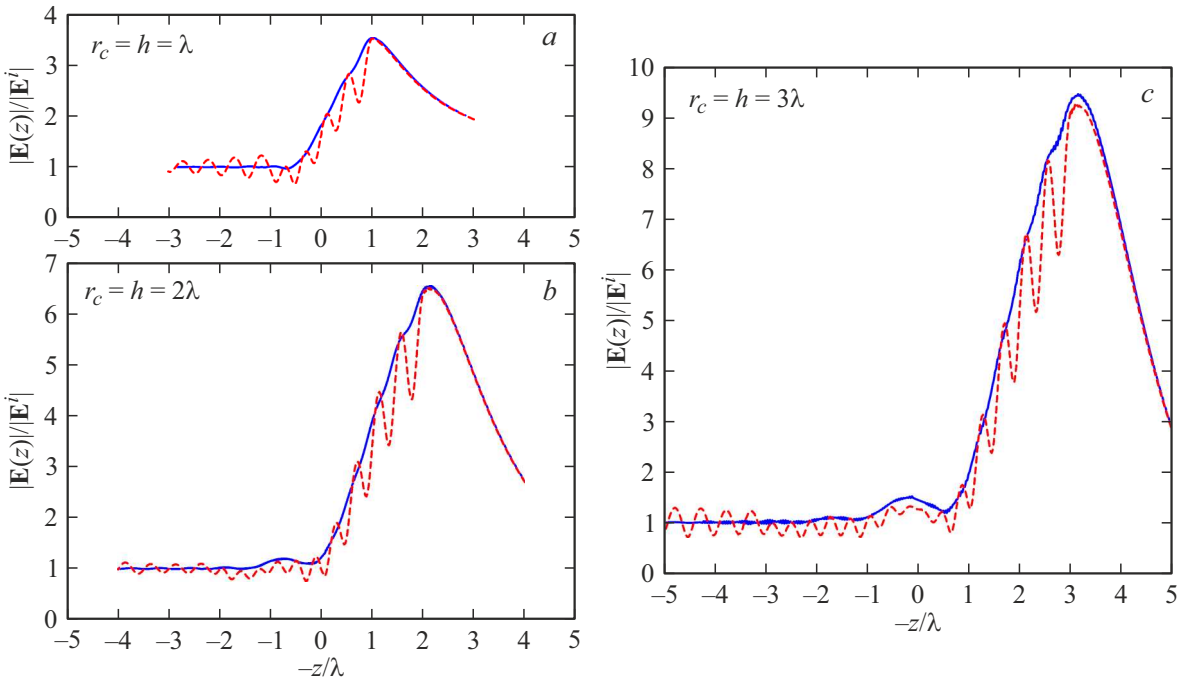

Figure 8. Field distribution along the axis of the Mikaelian lens of different radius $r_c = h$: solid lines — magneto-dielectric lens, dashed lines — dielectric lens.

The comparison showed that the calculation time with use of the new programs, at all other things being equal, was several times less than the calculation time taken in case of using the surface integral equation method. It was also demonstrated a decrease in the maximum field level in the focusing area due to replacement of the continuous refractive index profile by a stepped profile. The new programs were used for analysis of the effect of matching the surfaces for both types of the lenses with free space on the quality of focusing. Improved matching was achieved by use of magneto-dielectric material in the lenses with the same profiles of dielectric permittivity and magnetic permeability, which ensured that the wave resistance of the material was equal to the wave resistance of free space.

The obtained results demonstrate that the use of a magneto-dielectric material makes it possible to almost com-

pletely eliminate the wave reflection from the illuminated flat part of the lens surface, thus leading to increased field level in the focusing area compared to a purely dielectric lens. The indicated increase in the field level in the Mikaelian lens is less noticeable compared to the Maxwell lens, since the ideal matching in the Mikaelian lens is provided only in the direction of the normal to the flat surface in the focusing area. It is also shown that the Mikaelian lens, which has a longitudinal dimension equal to the transverse dimension, provides a higher field level in the focusing area compared to the Maxwell lens of the same transverse dimension.

Conflict of interest

The authors declare that they have no conflict of interest.

References

[1] J.C. Maxwell. The Cambridge and Dublin Mathematical J., **8**, 188 (1854).
[2] J.C. Maxwell. *Scientific Papers*, V. 1 (Cambridge University Press, 1890).
[3] A.L. Mikaelian. Doklady AN SSSR, **81** (4), 569 (1951).
[4] A.L. Mikaelian. In: *E. Wolf, Progress in Optics XVII* (North Holland, 1980).
[5] Z.L. Mei, J. Bai, T.M. Niu, T. Jun. IEEE Trans. Antennas Propag., **60** (1), 398 (2012).
[6] T. Baghdasaryan, T. Geernaert, H. Thienpont, F. Berghmans. IEEE Photon. J., **5** (4), 7100512 (2013).
[7] F. Maggiorelli, A. Paraskevopoulos, J.C. Vardaxoglou, M. Albani, S. Maci. IEEE Open J. Antennas and Propagation, **2**, 315 (2021).
[8] T. Whittaker, S. Zhang, A. Powell, C.J. Stevens, J.C. Vardaxoglou, W. Whittow. IEEE Antennas & Propagation Magazine, **65** (3), 10 (2023).
[9] E.I. Semernya, S.P. Skobelev. J. Opt. Soc. Am. A., **37** (12), 1873 (2020).
[10] E.I. Semernya, S.P. Skobelev. IEEE Antennas and Wireless Propagation Letters, **20** (2), 269 (2021).
[11] Ya.N. Feld, L.S. Benensen. *Antenno-fider devices*. Ch. 2 (Izd. VVIA named after Prof. N.E. Zhukovsky M., 1959) (in Russian).
[12] M. Born, E. Volf. *Foundations of optics*. 2-nd Edition. (Nauka, M., 1973) (in Russian).
[13] E.G. Zelkin, P.A. Petrova. *Lens antennas* (Sovetskoye radio, M., 1974) (in Russian).
[14] A.D. Greenwood, J.-M. Jin. IEEE Antennas & Propagation Magazine, **41** (5), 9 (1999).
[15] K. Boren, D. Khafmen. *Absorption and scattering of light by small particles* (Mir, M., 1986). (in Russian).
[16] P. Rozenfeld. IEEE Trans. Antennas Propag., **AP-24** (3), 365 (1976).

Translated by T.Zorina